Molecular mechanics studies of parallel and antiparallel phosphate-methylated DNA

Molecular Mechanics Studies of Parallel and Antiparallel Phosphate-Methylated DNA

MARCEL H. P. VAN GENDEREN,* LEO H. KOOLE, OLAV M. AAGAARD, COERT E. J. VAN LARE, and HENK M. BUCK,
Department of Organic Chemistry, Eindhoven University of Technology, 5600 MB Eindhoven, The Netherlands

Synopsis

Methylation of phosphate groups in oligo-dT strands leads to a parallel duplex with T · T base pairs. Molecular mechanics calculations on parallel d(TTTTTT)$_2$ show it to be a symmetric right-handed helix with B-DNA conformational characteristics. Phosphate methylation stabilizes the duplex by ca. 41 kcal/mol, due to removal of the interstrand phosphate electrostatic repulsions. The chirality introduced with phosphate methylation is important for the molecular geometry, since R_P methylation predominantly influences the conformation around the ζ bond (P—$O_{3'}$), while S_P methylation mostly changes the α conformation (P—$O_{5'}$). This is also true in antiparallel helices with methylated phosphates, as is shown by molecular mechanics calculations on d(GCGCGC)$_2$. These results may be of relevance to protein–DNA interactions, where phosphate charges are also shielded. As the pro-S_P oxygen is most available in a right-handed helix, we suggest changes around the α bond to occur upon protein complexation, leading to a widening of the major groove in the d(GCGCGC)$_2$ duplex (from 12 to 13 Å) and reduced minor groove (from 6 to 5 Å).

INTRODUCTION

Recently we observed that thymidine oligomers in aqueous solution can form duplexes after methylation of the phosphate groups.[1,2] These duplex structures are based on symmetric T · T base pairing via two N_3—H $\cdots$ O_4 hydrogen bonds, from which it follows that the 5′ → 3′ directions of the backbones are parallel instead of antiparallel (Fig. 1). Since unmethylated thymidine strands show no association in water (Ref. 3, pp. 310–311), the stability of the neutral phosphate-triesterified duplexes is most likely based on the absence of interstrand phosphate–phosphate repulsions. A detailed ^{1}H-nmr conformational analysis of the miniduplex of phosphate-methylated d(TT) was performed for both the R_P and S_P diastereomers on phosphorus.[2] This revealed that parallel helices are formed for both isomers, which are right-handed, with predominantly the standard γ^+ and β^t conformations for the $C_{4'}$—$C_{5'}$ and $C_{5'}$—$O_{5'}$ backbone bonds, and South sugar puckers. Via model building with computer graphics it was concluded that the helix is remarkably slim and has about 8 residues per turn.

In order to study this remarkable structure, we performed molecular mechanics calculations on the phosphate-methylated duplex d(TTTTTT)$_2$ with both R_P and S_P configurations on phosphorus[4] (Fig. 2). Since both R_P and S_P

*To whom correspondence should be addressed.

Biopolymers, Vol. 26, 1447–1461 (1987)

CCC 0006-3525/87/091447-15$04.00

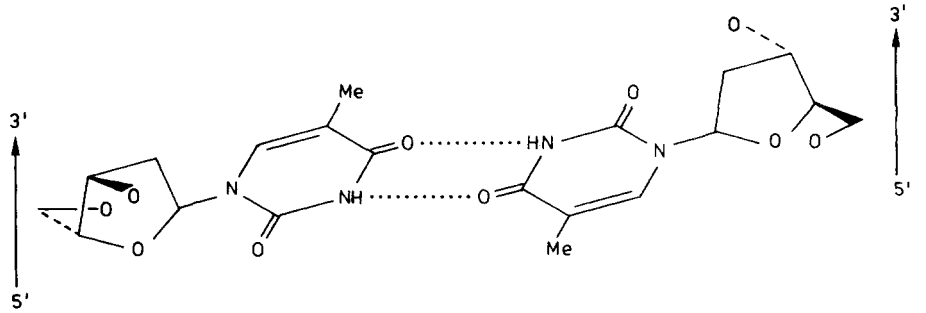

Fig. 1. Structure of the parallel T · T base pair with 5′ → 3′ backbone directions running in the same direction.

forms of phosphate-methylated d(TT)$_2$ have similar β, γ, and sugar conformations,[2] the difference in phosphate configuration should only influence the bonds near phosphorus (e.g., P—$O_{5'}$ or P—$O_{3'}$). The stability of the parallel duplex in relation to methylation was investigated by comparison with the unmethylated d(TTTTTT)$_2$ structure. It should be noted that this latter structure does not exist and is only used as a reference compound in the calculations.

The duplex formation of d(TTTTTT)$_2$ suggests that neutralization of the phosphate groups can influence DNA structures in general. Since such a neutralization will also occur (partially) in DNA–protein interactions that proceed via electrostatic interactions between amino acid side chains (e.g., arginine or lysine) and phosphates (Ref. 3, pp. 399–402), phosphate-methylated oligonucleotides can be used as simple models to study conformational changes in DNA after protein complexation. Therefore, we investigated the effects of R_P and S_P phosphate methylation on antiparallel DNA duplexes with molecular mechanics calculations on phosphate-methylated d(GCGCGC)$_2$. These results were compared with unmethylated d(GCGCGC)$_2$ duplexes.

METHODS

Calculations were carried out using the AMBER molecular mechanics program.[5] The energy function we used is conventional[6]:

$$E_{\text{total}} = \sum_{\text{bonds}} K_R(R - R_{\text{eq}})^2 + \sum_{\text{angles}} K_\theta(\theta - \theta_{\text{eq}})^2$$

$$+ \sum_{\text{dihedrals}} \frac{V_n}{2}[1 + \cos(n\phi - \gamma)] + \sum_{i<j}\left(\frac{A_{ij}}{R_{ij}^{12}} - \frac{B_{ij}}{R_{ij}^{6}} + \frac{q_i q_j}{\epsilon R_{ij}}\right)$$

$$+ \sum_{\text{H bonds}}\left(\frac{C_{ij}}{R_{ij}^{12}} - \frac{D_{ij}}{R_{ij}^{10}}\right)$$

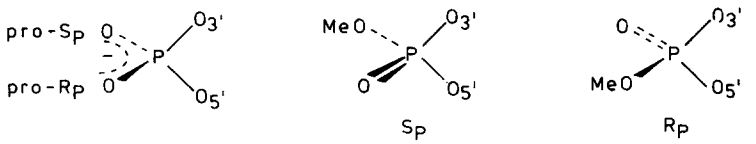

Fig. 2. Definition of R_P- and S_P-methylated phosphate triesters, and of the pro-R_P and pro-S_P nomenclature in the phosphate diester.

All degrees of freedom were energy refined until the rms of the energy gradient was less than or equal to 0.1 kcal/mol/Å. For all calculations, the united-atom approach was used first. Subsequently, hydrogen atoms were added and an all-atom energy refinement was carried out. The force constants and equilibrium values were initially taken as previously described,[6] but changes were made in input parameters and force field for calculations on phosphate-methylated systems (*vide infra*). The dielectric constant ϵ was set at R_{ij} in all calculations, to mimic the damping effect of the solvent on electrostatic interactions. Since we were especially interested in effects of phosphate neutralization, we also performed calculations with sodium counterions for unmethylated structures. The ions were located at a distance of 5 Å from phosphorus, and at equal distances from the two nonbridging phosphate oxygens.

Changes in Input Parameters

For phosphate-methylated substrates, we defined new phosphate groups with the PREP module,[5] incorporating a methyl group on one of the nonbridging oxygens. The types and charges of the atoms in the phosphate group were adjusted to reflect this triesterification (Table I). The coordinates of all units are those of Arnott et al.,[7] and a methyl group was added on one phosphate oxygen with a torsion angle of +60° relative to the P=O bond, a C—O bond length of 1.44 Å, and a P—O—C angle of 120°. For the construction of the parallel helix geometry, we started by building an antiparallel $d(TTTTTT)_2$ helix with the NUCGEN module.[5] Elimination of one strand and doubling the remaining one by a rotation of 180° around the helix axis afforded a reasonable starting geometry (manipulations performed with the

TABLE I
Input Parameters for Unmethylated, R_P-Methylated, and S_P-Methylated Phosphate Groups

	Standard[a]		R_P Methylated		S_P Methylated	
Atom	Type	Charge	Type	Charge[b]	Type	Charge[b]
P	P	1.429	P	0.680	P	0.680
$O_{5'}$	OS	−0.535	OS	−0.292	OS	−0.292
$O_{3'}$	OS	−0.535	OS	−0.292	OS	−0.292
$O_{pro\text{-}S_P}$	O2	−0.850	O	−0.356	OS	−0.292
$O_{pro\text{-}R_P}$	O2	−0.850	OS	−0.292	O	−0.356
C_{methyl}	—	—	C3[c]	0.211	C3[c]	0.211

[a] Taken from Ref. 6.
[b] Based on *ab initio* (Gaussian-80 STO-3G) calculations of trimethylphosphate.
[c] For the all-atom approach, replace by CT (charge −0.047) and three HCs (charge 0.091).

TABLE II
Force Field Potentials for Phosphate-Methylated DNA

Bonds	R_{eq}[a]	K_R[b]		Angles	θ_{eq}[c]	K_θ[d]	
P—O	1.435	625.0		O—P—OS	117.4	125.0	
Torsions	$\frac{V_n}{2}$[e]	n	γ	Torsions[f]	$\frac{V_n}{2}$[e]	n	γ
O—P—OS—C3	0.25	3	0	OS—P—OS—C3	0.25	3	0
O—P—OS—C3	0.75	2	0	OS—P—OS—C3	0	2	0
O—P—OS—C2	0.25	3	0	OS—P—OS—C2	0.25	3	0
O—P—OS—C2	0.75	2	0	OS—P—OS—C2	0	2	0
O—P—OS—CH	0.25	3	0	OS—P—OS—CH	0.25	3	0
O—P—OS—CH	0.75	2	0	OS—P—OS—CH	0	2	0
O—P—OS—CT[g]	0.25	3	0	OS—P—OS—CT[g]	0.25	3	0
O—P—OS—CT[g]	0.75	2	0	OS—P—OS—CT[g]	0	2	0

[a] Bond length in Å.
[b] Bond stretching parameter in kcal/mol/Å^2.
[c] Bond angle in degrees.
[d] Bond angle deformion parameter in kcal/mol/rad^2.
[e] Torsional barrier in kcal/mol.
[f] Only in FF2.
[g] Only for all-atom approach.

Chem-X program*), even though the thymine bases are separated by a large distance (N_3—O_4 distance is 4.70 Å instead of the required 2.84 Å[1]). This helix geometry was used instead of the standard NUCGEN output.

Changes in the Force Field

New potentials were defined for the phosphate triester group. First, bond stretching and bond-angle deformation parameters for the new P=O bond were introduced. The value of R_{eq} was taken as 1.435 Å, based on x-ray data.[8] Linear extrapolation of the force constants of the P—O_{ester} and P—O^- bonds[7] suggested a K_R value of 625.0 kcal/mol/Å^2 for the P=O bond. The equilibrium bond angle O—P=O was set at θ_{eq} = 117.4°, based on our own *ab initio* calculations on trimethylphosphate. A force constant K_θ of 125.0 kcal/mol/rad^2 was derived by comparison with the other O—P—O angles.[6] For the torsion angles in the O=P—O—C fragments, specific three- and twofold potentials were introduced, similar to the existing O—P—O—C potentials[6] ($V_3/2$ = 0.25 kcal/mol, γ = 0; and $V_2/2$ = 0.75 kcal/mol, γ = 0). This results in a force field (FF1) that was used initially (Table II). Taking into account the well-known predominance of the P=O bond over P—O bonds in determining phosphate conformations,[9] a second change produced a force field (FF2) without specific twofold potentials for O—P—O—C fragments (Table II). This results in a tendency for *gauche* orientation relative to the P=O bond, instead of the earlier preference of *gauche* orientation to the P—O_{ester} bonds. However, the FF1 results already showed conformational effects due to the P=O bond, and the use of FF2 did

*Copyright: Chemical Design Ltd., Oxford.

not produce large changes in the geometries. For the FF2 calculations, we did find a lower total energy (since one torsional energy term is removed), but stabilities remained essentially the same when expressed as the total interstrand energy. In the case of unmethylated systems, FF1 is identical to the initial force field,[6] and we therefore present the FF1 results. We feel the FF2 force field gives a more accurate description for the methylated duplexes, and discuss FF2 results for these systems. It must be stressed, however, that both force fields have been used on all systems, and that the resulting geometries and stabilities are virtually independent of the choice of force field.

RESULTS AND DISCUSSION

Parallel d(TTTTTT)$_2$

The parallel input structure contracted appreciably (ca. 25% in volume) during the energy optimization to fit the T · T hydrogen bonds. The resulting structures for the two unmethylated duplexes (with and without counterions) and the two methylated duplexes (R_P and S_P configurations) display conformations well within the ranges for standard B-DNA, as can be seen in Table III and Fig. 3.

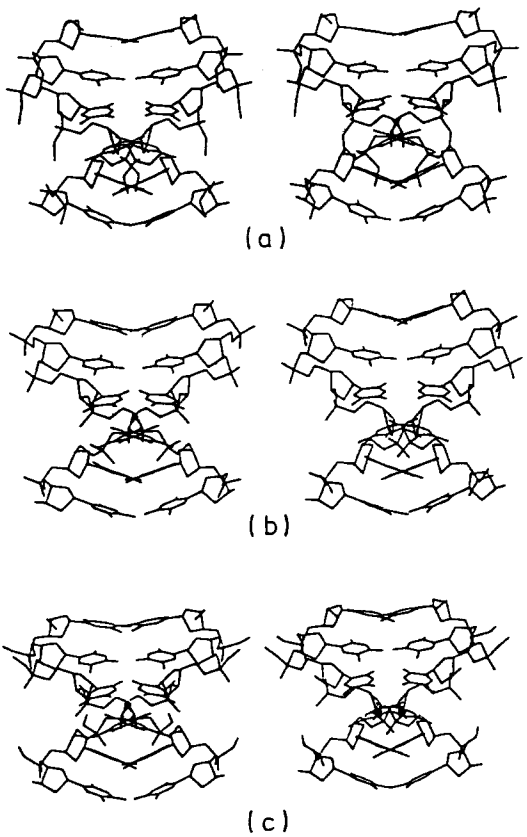

Fig. 3. Stereoview of the minimized structures for the R_P-methylated (a), unmethylated (b), and S_P-methylated (c) d(TTTTTT)$_2$ duplexes.

TABLE III
Conformational Characteristics[a] of the d(TTTTTT)$_2$ Systems

System	α[b] (P—$O_{5'}$)	β ($O_{5'}$—$C_{5'}$)	γ ($C_{5'}$—$C_{4'}$)	δ ($C_{4'}$—$C_{3'}$)	ϵ ($C_{3'}$—$O_{3'}$)	ζ ($O_{3'}$—P)	χ ($C_{1'}$—N)	P[c]	ψ_m[c]	hra[d]
Unmethylated	−69.5	167.0	65.4	115.3	181.9	−89.5	−125.0	124.5	40.0	40.4
Counterions	−68.1	167.3	63.0	114.5	182.0	−88.4	−131.6	120.6	40.0	38.3
R_P methylated	−63.1	165.2	63.0	116.0	184.6	−95.7	−125.5	121.4	40.0	40.8
S_P methylated	−61.5	164.1	61.6	112.0	183.0	−88.4	−124.7	122.8	40.0	40.9

[a]Average of the four inner base pairs.
[b]Torsion angles in degrees. Definitions are according to IUPAC-IUB recommendations.[10]
[c]Pucker phase and pucker amplitude in degrees, according to the pseudorotation concept of Altona and Sundaralingam.[11]
[d]Helical repeat angle in degrees.

TABLE IV
Total Energies and Energy Contributions in the d(TTTTTT)$_2$ Systems

System	E_{tot}[a]	E_{bond}[b]	E_{angle}[c]	$E_{torsion}$[d]	E_{VDW}^{1-4}[e]	E_{VDW}^{nb}[f]	E_{EEL}^{1-4}[g]	E_{EEL}^{nb}[h]	$E_{H\ bond}$[i]	E_{inter}[j]
Unmethylated	−321.00	5.36	47.19	103.73	62.71	−177.52	−563.50	206.76	−5.75	−67.20
Counterions	−519.52	5.21	46.44	105.06	62.37	−189.86	−562.85	18.95	−4.84	−95.27
R_P methylated	−343.28	5.39	46.94	122.89	66.16	−185.01	−428.45	34.63	−5.84	−108.83
S_P methylated	−334.97	5.30	46.87	128.87	64.91	−181.62	−428.45	35.97	−6.83	−107.89

[a]Total energy. All energies in kcal/mol.
[b]Bond stretching energy.
[c]Angle deformation energy.
[d]Torsional energy.
[e]Vicinal van der Waals energy.
[f]Nonbonded van der Waals energy.
[g]Vicinal electrostatic energy.
[h]Nonbonded electrostatic energy.
[i]Hydrogen-bond energy.
[j]Interstrand energy.

TABLE V
Interstrand Energy[a] of d(TTTTTT)$_2$ Duplexes as a Function of ϵ

System	$\epsilon = R_{ij}$	$\epsilon = 4$	$\epsilon = 2$	$\epsilon = 1$
Unmethylated	−67.20	66.14	177.79	401.09
Counterions	−95.27	4.98	56.81	160.47
R_P methylated	−108.83	−69.57	−93.39	−141.01
S_P methylated	−107.89	−65.84	−84.04	−120.44

[a] In kcal/mol.

The backbone conformations β^t and γ^+ are found, as well as $C_{1'}$-*exo* deoxyribose puckers (P ≈ 122°), which agrees with the experimental data. Aside from end effects, the helices are very regular and highly symmetric with respect to the helix axis with two identical grooves. A rather large helical repeat angle of ca. 40°, or a ninefold helix symmetry, also agrees with the earlier preliminary model studies, which suggested an eightfold symmetry in this svstem.

The energy contributions (Table IV) clearly show a diminished electrostatic energy after methylation. The long-distance term E^{nb}_{EEL} is especially responsible for this decrease, which reflects the removal of phosphate–phosphate repulsions. The interstrand interaction energy (E_{inter}), which we use to quantify the stability of the duplex, decreases ca. 18 kcal/mol for the counterion system and ca. 41 kcal/mol after methylation of the phosphates. Therefore, it can be concluded that shielding of the phosphate charges indeed leads to a more stable duplex. Although all four systems have a negative interstrand energy, analysis of the stability with various values of ϵ indicates that only the neutral duplexes remain stable (Table V) when electrostatic interactions are enhanced at low ϵ.

In the unmethylated systems, the increased electrostatic repulsion destabilizes the duplex, even when counterions are present. For the methylated systems, the stability even increases on going from $\epsilon = 4$ to $\epsilon = 1$, indicating that electrostatic attractions are dominant.

In an interaction diagram (Fig. 4), it can be seen that the T · T base pairs have a binding energy of 11 kcal/mol, and stacking accounts for 6 kcal/mol (intrastrand) and 3 kcal/mol (interstrand). This does not change significantly upon methylation of the phosphates.

Addition of counterions has only a small effect on interstrand phosphate–phosphate (P–P) repulsions, but methylation reduces P–P interactions significantly. Due to the specific geometry of this parallel helix (helix diameter 18 Å, rise per turn 29 Å, 8–9 residues per turn, rotational twofold symmetry), P–P distances behave in an unusual way. Numbering the nucleotide units (with the 5′-phosphate included in the unit[11]) as follows:

1		2		3		4		5		6
T	-	T	-	T	-	T	-	T	-	T
T	-	T	-	T	-	T	-	T	-	T
7		8		9		10		11		12

it was seen that interstrand P–P distances decrease for the series 1–7, 1–8, 1–9, and 1–10, after which they increase for 1–11 and 1–12. This means that

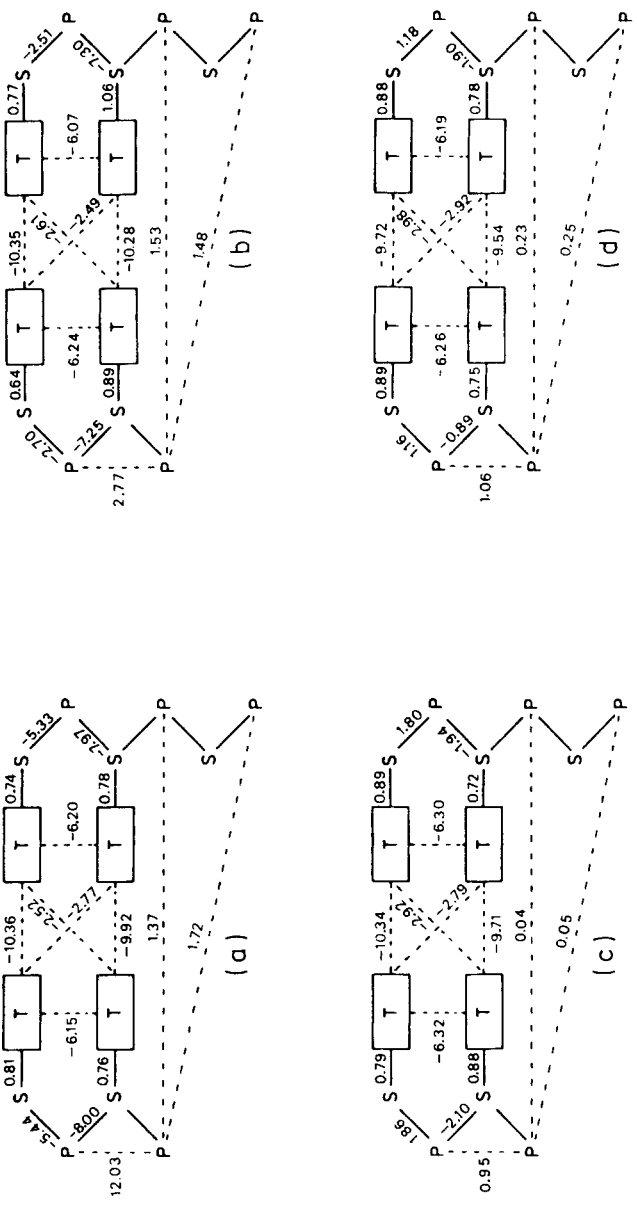

Fig. 4. Energy interaction scheme for the four d(TTTTTT)$_2$ systems: unmethylated (a), unmethylated with counterions (b), R_P methylated (c), and S_P methylated (d). For the unmethylated structure with counterions, the Na^+ ion is included in the phosphate group.

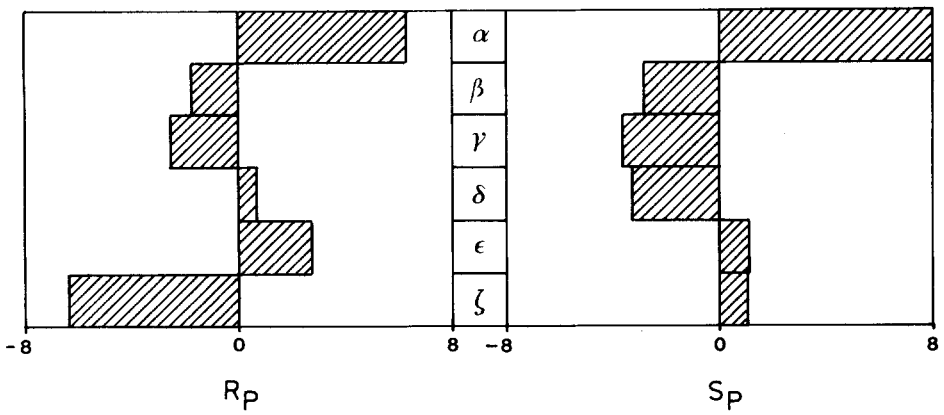

Fig. 5. Changes in the backbone torsion angles in R_P- and S_P-methylated d(TTTTTT)$_2$ relative to the unmethylated duplex.

P–P repulsions between 1 and 8–10 are more important than the 1–7 interaction on the same level in the helix. Fig. 4 shows that the diagonal P–P repulsion is indeed usually stronger than the horizontal one. In standard B-DNA (helix diameter 23 Å, rise per turn 33 Å, 10 residues per turn, strands form a major and minor groove), the interstrand P–P distance is always smallest between units on the same level in the helix and increases uniformly for phosphates in nucleotide levels on different levels. For the slim parallel helix it is therefore necessary to eliminate P–P repulsions over a length of many base pairs to achieve stability.

Concerning the differences between R_P and S_P configuration on phosphorus, it can be seen that the stabilities are almost equal (Table IV). However, certain conformational differences between the two methylated duplexes are apparent, especially for the α (P—$O_{5'}$) and ζ (P—$O_{3'}$) bonds (Fig. 5). In the all-atom calculations, the tight parallel helix has little conformational freedom and differences are small (up to ca. 8°).

Still, it is clear that R_P methylation influences the α and ζ conformations, while in the S_P form mostly changes around the α-bond are seen. That the chirality of phosphorus is important in determining the conformation of the DNA helix led us to investigate the effects of methylation in d(GCGCGC)$_2$. We feel methylation may be relevant in studying complexation of proteins with backbone phosphates (*vide supra*). If interaction proceeds with one phosphate oxygen only, this could then be translated into stereospecific conformational changes.

Antiparallel d(GCGCGC)$_2$

The antiparallel input structures did not change much during energy refinement. Table VI shows that conformations for all four systems are in the expected range for right-handed helices.

Sugar puckers are $C_{2'}$-*endo* (P ≈ 145°) and helical repeat angles indicate a nine- to tenfold symmetry. The effect of phosphate methylation is a decrease of nonbonded electrostatic energy and a stabilization of the helix of ca. 34

kcal/mol (Table VII). Addition of counterions leads to a stabilization of ca. 8 kcal/mol.

In an interaction diagram (Fig. 6), it can be seen that the interstrand phosphate–phosphate repulsions decrease appreciably in the methylated systems. As discussed before, P–P interactions on the same level are more important than P–P repulsions between units on different levels (*vide supra*). The guanine and cytosine bases have an interaction energy of ca. 22 kcal/mol, and stacking interactions follow the usual pattern.[12] Guanine on the 5′ side of cytosine gives an interaction of ca. 10 kcal/mol, and guanine on the 3′ side of cytosine gives ca. 7 kcal/mol. There is a difference between the R_P- and S_P-methylated forms concerning the stacking interactions, since in the R_P form the intrastrand stacking is stronger by 1 kcal/mol. This was suggested earlier by Kan et al.[13] for methylphosphonate dinucleotides on the basis of model building. We can now offer an explanation for this effect (*vide infra*). Analysis of E_{inter} with various values of ϵ (Table VIII) shows that only the methylated systems remain stable, while the unmethylated systems become unstable at low ϵ, as was also seen for the parallel systems.

Focusing upon the different conformations of the R_P- and S_P-methylated duplexes, a clear effect on ζ and α can be seen compared to the unmethylated system (Fig. 7), since in the $d(GCGCGC)_2$ duplexes more conformational freedom is present compared to the parallel helices (changes up to ca. 16°). Again we see the correlations R_P-ζ and S_P-α.

These results are in good accord with the expected conformational changes upon introducing a P=O bond. Depending upon which phosphate oxygen bears a methyl group, one of the $P—O_{ester}$ bonds tends to change its unfavorable conformation with the O—C bond *trans* to the P=O bond[9] (Fig. 8). It can be seen that this causes a specific relation between chirality and conformational change.

The overall effect of the conformational changes around α or ζ bonds is obvious when one takes into account that the ζ bond is located along the helix axis, whereas the α bond is nearly at right angles with the axis. Changes around ζ will therefore lead to longitudinal motions, and variations around α will lead to transversal motions. As can be seen in Fig. 9, these effects are indeed present. In the R_P-methylated system, a small transversal shift for each base pair is seen, which is the reason for the differences in stacking interactions between the R_P and S_P forms (*vide supra*). A different and larger effect is observed in the S_P-methylated duplex, where a longitudinal change in the backbones occurs. The strands approach each other, since P–P repulsions are virtually eliminated and a widening of the major groove results from 12 to 13 Å. The minor groove diminishes in size from 6 to 5 Å because of this process (see Fig. 10).

In a model of right-handed DNA, the pro-S_P oxygen in the phosphate group is seen to be located at the periphery of the helix, whereas the pro-R_P oxygen resides in the major groove. This suggests that the pro-S_P oxygen will be the specific recognition site for protein interactions, as is confirmed by experiments with the Ada enzyme from *E. coli*.[14] This protein removes only methyl groups from S_P-methylated phosphates in ds-DNA. If one assumes that the pro-S_P oxygen will be shielded by a protein in the $d(GCGCGC)_2$ duplex,

TABLE VI
Conformational Characteristics[a] of the d(GCGCGC)$_2$ Systems

System	α (P—$O_{5'}$)	β ($O_{5'}$—$C_{5'}$)	γ ($C_{5'}$—$C_{4'}$)	δ ($C_{4'}$—$C_{3'}$)	ϵ ($C_{3'}$—$O_{3'}$)	ζ ($O_{3'}$—P)	χ ($C_{1'}$—N)	P	ψ_m	hra
Unmethylated	−72.6	178.2	61.5	143.1	183.6	−113.7	−115.1	155.6	41.0	38.6
Counterions	−69.7	174.5	58.5	127.4	184.4	−99.3	−123.1	136.1	39.0	35.1
R_P methylated	−72.6	171.4	60.7	136.9[b]	187.8	−102.2	−112.8	155.4[b]	39.0	36.8
S_P methylated	−57.9	172.4	57.9	139.9	180.6	−115.6	−120.0	154.0	40.0	41.9

[a]Average of all base pairs. See also footnotes to Table III.
[b]The cytosine sugar torsion angles are excluded, due to high variability (P and δ range from 97° to 140°).

TABLE VII
Total Energies and Energy Contributions in the d(GCGCGC)$_2$ Systems

System	E_{tot}	E_{bond}	E_{angle}	$E_{torsion}$	E_{VDW}^{1-4}	E_{VDW}^{nb}	E_{EEL}^{1-4}	E_{EEL}^{nb}	$E_{H\ bond}$	E_{inter}
Unmethylated	−523.55	4.60	50.23	110.57	59.29	−185.73	−1114.04	553.09	−1.57	−121.20
Counterions	−710.63	4.29	46.05	109.79	60.93	−200.91	−1115.08	386.21	−1.92	−129.22
R_P methylated	−539.04	4.23	48.65	124.39	63.83	−196.99	−977.09	395.82	−1.88	−153.33
S_P methylated	−519.58	4.49	48.18	142.57	63.34	−197.45	−979.32	402.08	−1.46	−158.00

[a]Energies in kcal/mol. See also footnotes to Table IV.

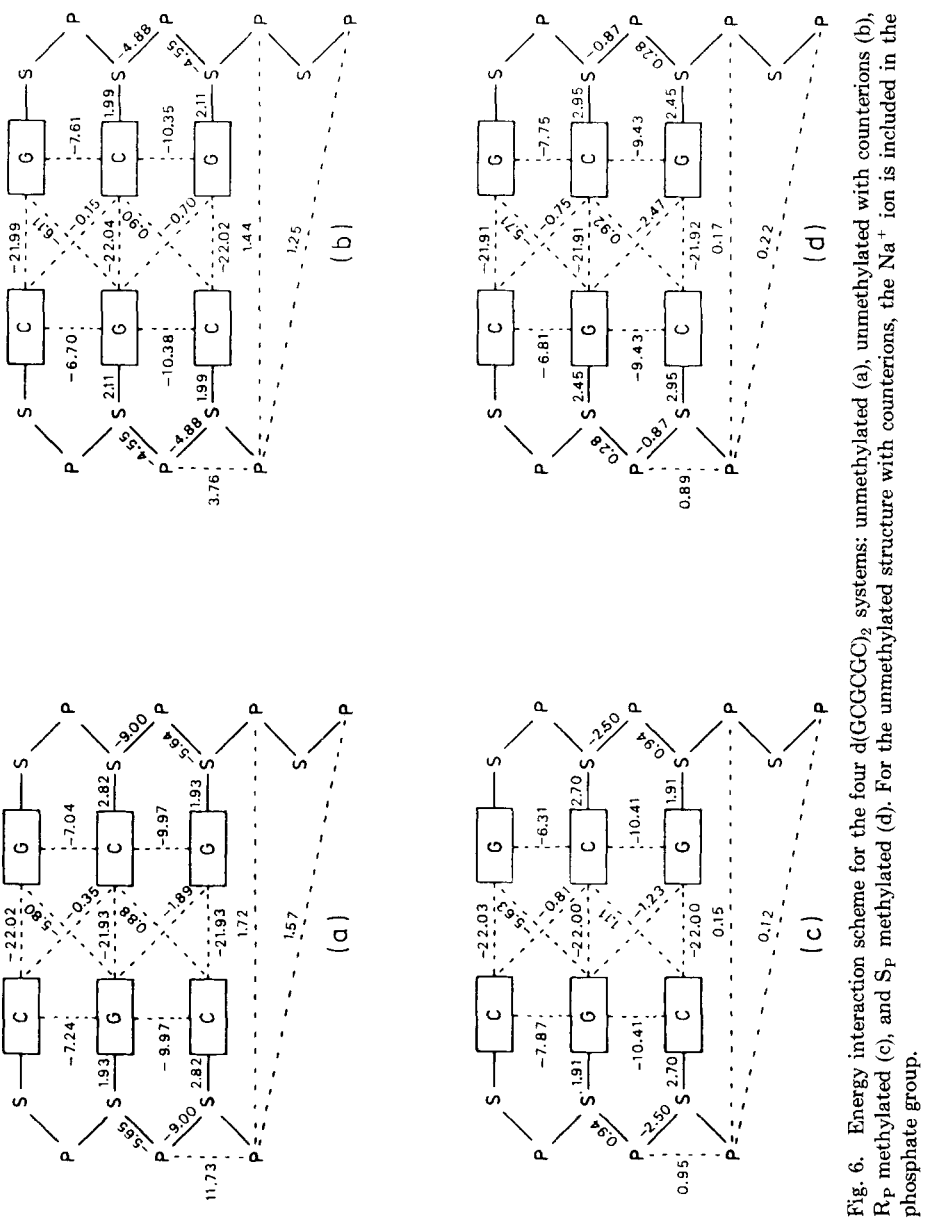

Fig. 6. Energy interaction scheme for the four $d(GCGCGC)_2$ systems: unmethylated (a), unmethylated with counterions (b), R_P methylated (c), and S_P methylated (d). For the unmethylated structure with counterions, the Na^+ ion is included in the phosphate group.

TABLE VIII
Interstrand Energy[a] of the d(GCGCGC)$_2$ Duplexes as a Function of ϵ

System	$\epsilon = R_{ij}$	$\epsilon = 4$	$\epsilon = 2$	$\epsilon = 1$
Unmethylated	−121.20	48.61	143.23	332.58
Counterions	−129.22	18.64	81.73	207.90
R_P methylated	−153.33	−69.90	−94.47	−143.61
S_P methylated	−158.00	−71.71	−93.21	−136.15

[a] In kcal/mol.

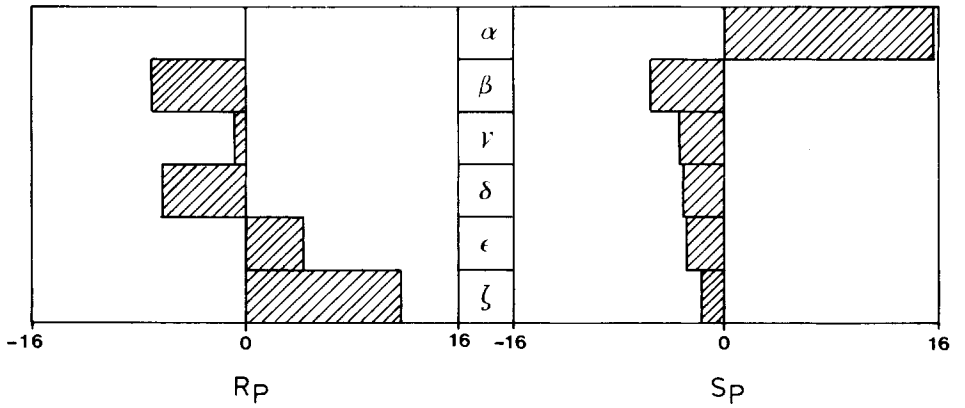

Fig. 7. Changes in the backbone torsion angles in R_P- and S_P-methylated d(GCGCGC)$_2$ relative to the unmethylated duplex.

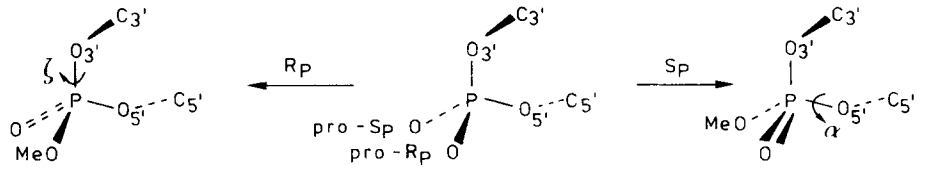

Fig. 8. Expected changes in the α and ζ bonds upon R_P or S_P triesterification of the phosphate group. Both $C_{3'}$ and $C_{5'}$ prefer a *gauche* orientation to the P=O bond.

conformational changes in the α bond are expected. According to our results, this will then lead to a widening of the major groove of the helix.

CONCLUDING REMARKS

The calculated structures and stabilities of the parallel helix of d(TTTTTT)$_2$ are in good agreement with our earlier experimental data. Methylation of the phosphate groups increases the stability of the slim helix by elimination of the interstrand phosphate–phosphate repulsions. The difference between R_P and S_P configuration in the phosphate triester is mainly reflected in the ζ resp. α conformations. As we found experimentally, the stabilities and the β, γ, and sugar conformations (which can be determined with ^{1}H-nmr) are virtually not influenced by the orientation of the methyl group. A different situation is found for phosphate triesters with ethyl groups,[15] where the orientation of the

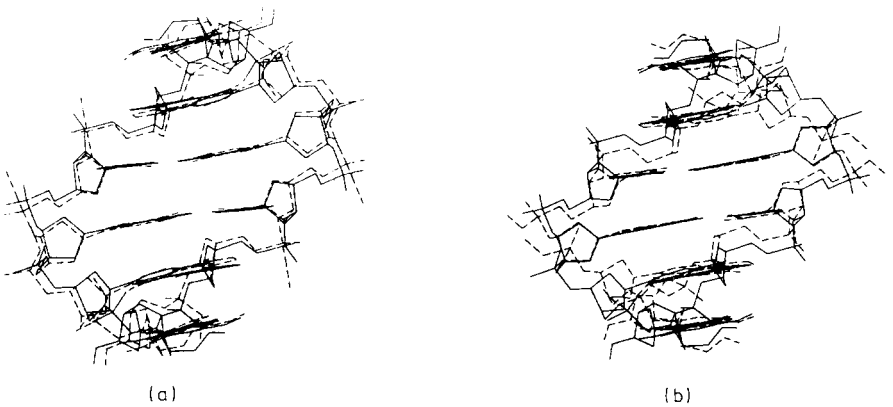

Fig. 9. Overall changes in the d(GCGCGC)$_2$ helix for R_P methylation (a) and S_P methylation (b). Drawn lines depict the unmethylated structure, while dashed lines refer to the methylated structures.

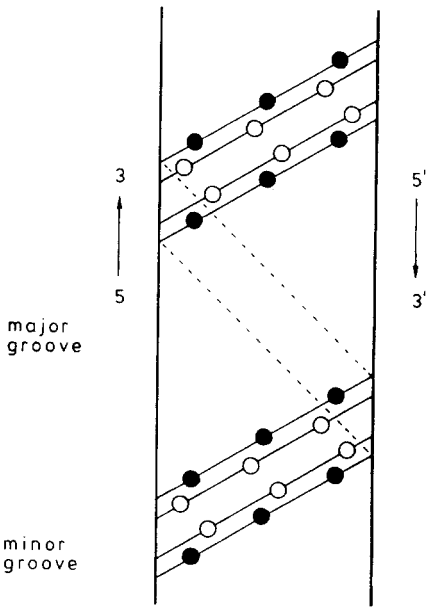

Fig. 10. Schematic description of the changes in the grooves for the S_P-methylated helix structure. The positions of the phosphate groups are indicated with • for the unmethylated system, and ○ for the S_P-methylated duplex.

more bulky ethyl moieties does have a strong influence on the duplex formation.

In antiparallel DNA, phosphate methylation also induces specific conformational changes dependent on phosphate configuration. Considering this neutralization of the phosphate groups as a model for protein–DNA interactions, we conclude that complexation with the (best available) pro-S_P oxygen results in a larger major groove (ca. 10%) and smaller minor groove (ca. 20%) in the

d(GCGCGC)$_2$. This process may be important for DNA–protein recognition, since the nucleobases are now more exposed to the surroundings of the helix. Oligonucleotide systems with different length and sequences will be investigated to see the general impact of phosphate shielding on DNA conformations.

This investigation was supported in part by the Netherlands Foundation for Chemical Research (SON), with financial aid from the Netherlands Organization for the Advancement of Pure Research (ZWO). Use of the services and facilities of the Dutch CAOS/CAMM Center, under grant numbers SON-11-20-700 and STW-NCH-44.0703, is gratefully acknowledged. We wish to thank Dr. J. Noordik (CAOS/CAMM Center) and Mr. M. Blommers (Catholic University of Nijmegen, The Netherlands) for helpful discussions.

References

1. Koole, L. H., van Genderen, M. H. P., Frankena, H., Kocken, H. J. M., Kanters, J. A. & Buck, H. M. (1986) *Proc. Kon. Ned. Akad. van Wetensch.* **B89**, 51–55. (Communicated by H. M. Buck at the meeting of November 25, 1985.)

2. Koole, L. H., van Genderen, M. H. P. & Buck, H. M. (1987) *J. Am. Chem. Soc.*, in press.

3. Saenger, W. (1984) *Principles of Nucleic Acid Structure*, Springer Verlag, New York.

4. Cahn, R. S., Ingold, C. & Prelog, V. (1966) *Angew. Chem.* **78**, 413–447.

5. Weiner, P. K. & Kollman, P. A. (1981) *J. Comp. Chem.* **2**, 287–303.

6. Weiner, S. J., Kollman, P. A., Case, D. A., Singh, U. C., Ghio, C., Alagona, G., Profeta, S., Jr. & Weiner, P. K. (1984) *J. Am. Chem. Soc.* **106**, 765–784.

7. Arnott, S., Campbell-Smith, P. & Chandresekaharan, P. (1976) in *CRC Handbook of Biochemistry and Molecular Biology, Nucleic Acids*, Vol. 2, Fasman, G. D., Ed., CRC, Cleveland, OH, pp. 411–422.

8. Kennard, O., Watson, D. G., Allen, F. H., Isaacs, N. W., Motherwell, W. D. S., Pettersen, R. C. & Town, W. G., Eds. (1972) *Molecular Structures and Dimensions*, Vol. A1, A. Oosthoek's Uitgevers, Utrecht, pp. 274–276.

9. Hayes, D. M., Kollman, P. A. & Rothenburg, S. (1977) *J. Am. Chem. Soc.* **99**. 2150–2154.

10. IUPAC–IUB Commission on Biochemical Nomenclature (1983) *Eur. J. Biochem.* **131**, 9–15.

11. Altona, C. & Sundaralingam, M. (1973) *J. Am. Chem. Soc.* **94**, 8205–8212.

12. Kollman, P. A., Weiner, P. K. & Dearing, A. (1981) *Biopolymers* **20**, 2583–2621.

13. Kan, L. S., Cheng, D. M., Miller, P. S., Yano, J. & Ts'o, P. O. (1980) *Biochemistry* **19**, 2122–2132.

14. Hamblin, M. R. & Potter, B. V. L. (1985) *FEBS Lett.* **189**, 315–317.

15. Pless, R. C. & Ts'o, P. O. P. (1977) *Biochemistry* **16**, 1239–1250.

Received December 22, 1986
Accepted March 10, 1987